Title: Eukaryotic Microbial Richness Increases with Latitude and Decreasing Temperature in the Pacific Subarctic Domain in Late Winter

Final draft version, some editing in the final published version NOT included.

Published version accessible in Polar Biology:

https://link.springer.com/article/10.1007/s00300-017-2131-2

Running title: Bering Sea eukaryotic microbial diversity

Byline: B.T. Hassett[1,#], R. Gradinger[1,2]

Affiliation: [1]University of Alaska Fairbanks, School of Fisheries and Oceanography, PO Box 757220, Fairbanks, AK 99775-7220, U.S.A.**;** [2] Institute of Marine Research, Postboks 6404, N-9294, Tromsø, Norway.

Correspondence to: Brandon T. Hassett, UAF SFOS, PO Box 757220 Fairbanks, AK 99775; (907) 474-5011; bhassett@alaska.edu

Abstract: The Bering Sea has some of the highest concentrations of inorganic nutrients of any marine system. In the Bering Sea, eukaryotic microbes interface inorganic nutrient sequestration and cycling processes that drive one of the most productive ecosystems globally. Historical surveys of eukaryotic diversity in the Bering Sea have relied on microscopy and culturing-dependent analyses to assess microbial diversity patterns. In this study, we used high-throughput sequencing (Illumina MiSeq) of the 18S rRNA gene to explore general patterns of eukaryotic diversity from six regions in the Bering Sea and surrounding Subarctic Pacific. The greatest richness was found in the Shelikof Strait and at the marginal ice zone. The lowest richness was found in the deep water basin south of the Aleutian Islands. Ordination analysis of our sequences revealed nearly identical community structures between our Shelikof Strait and the deep water basin sites. Operational taxonomic unit analysis revealed that water samples from the Bering Sea sites shared more OTUs with the Shelikof Strait site than with the sea ice sample, despite the existence of sea ice in the Bering Sea, reflecting known circulation patterns out of the Gulf of Alaska. Richness increased with increasing latitude and decreasing temperature, suggesting that the base of food webs is susceptible to temperature perturbations.

Keywords: 18S rRNA, Bering Sea, Aleutian Islands, chlorophyll maximum, Phosphate, Silicate

Introduction: Microbes are the foundation of all marine food webs and catalyze essential biogeochemical cycling throughout the world's oceans. Microbes comprise 90% of all living oceanic biomass (Suttle 2007), yet are proportionally understudied in the Arctic and Subarctic (Gradinger et al. 2010). As high-latitude seas continue to warm, the metabolic activity and structure of microbial communities are likely to change, favoring organisms genetically capable of coping with elevated temperatures (Steele 2008), fluxes within the nutrient regime (Doney et al. 2012), and biological competition due to range extensions of boreal taxa, as established for several trophic levels within Subarctic and Arctic seas (Fossheim et al. 2015; Meuter and Litzow 2008). As microbes differentially respond to environmental perturbations (Comeau et al. 2011), future community equilibriums remain uncertain, owed in part to the lack of contemporary species inventories and the understudied nature of abiotic drivers involved in shaping large-scale microbial diversity patterns.

In general, organismal diversity gradients within high-latitude seas are known to differ along longitudinal (Piepenburg et al. 2011) and latitudinal axes (Yasuhara et al. 2012), driven by a combination of evolutionary history (Galand et al. 2009) and seasonal physical forcing (Carmack et al. 2006). Physical forcing in the Subarctic and Arctic is particularly strong on diversity patterns, governed by the extreme seasonality of light (Gradinger 2009), and temporally and spatially changing nutrient concentrations (Holmes et al. 2012) that regulate the phenology of photosynthetic primary production of ice algae and phytoplankton (Leu et al. 2015). Additionally, the seasonally-increasing marine primary productivity in Polar Regions stimulates and regulates microbial community diversity patterns (Hodges et al. 2005; Roy et al. 1998).

The Bering Sea is a semi-enclosed high-latitude sea, consisting of a deep central basin with surrounding continental shelves. Circulation patterns in the Bering Sea are driven by the Alaskan Coastal Current and the eastward flowing Aleutian North Slope current that moves northwestwardly (as the Bering Slope current) and finally southwardly (as the Kamchatka Current) near Russia. This anticyclonic flow of water forms part of the North Pacific Subarctic Gyre (Stabeno et al. 1999). High production on the northern Bering Sea shelf is supported by the continuous advection of nutrient-rich waters, while the southeastern shelf depends on cross-shelf exchanges (Aydin and Meuter 2007). The continental shelf of the eastern Bering Sea is one of the most productive marine ecosystems in the world (Mueter and Litzow 2008) that is experiencing significant warming (Stabeno et al. 2001). Increased warming on continental shelves should lead to a northward migration of the Arctic-Subarctic ecotone (Mueter and Litzow 2008).

The rapid growth rate of microorganisms (relative to zooplankton or larger metazoans) allows microbial communities to rapidly shift into different equilibrium states, serving as useful indicator organisms for environmental change (Comeau et al. 2011). Historically, culturing-based studies (e.g. Hassett et al., 2015) and microscopy (e.g. Szymanski and Gradinger 2016) were used to assess eukaryotic microbial diversity in the Bering Sea. In this study, we applied high-throughput sequencing (HTS) techniques to explore general patterns of eukaryotic diversity from the Bering Sea region and the relationship of these patterns with the physical environment. We hypothesized that the eukaryotic microbial community structure would differ with hydrography, possibly indicating temperature-induced changes in the microbial population. We also hypothesized that the nutrient-rich waters of the Bering Sea would be a significant driver of microbial community structure, favoring the growth of specific microbial clades.

Materials and Methods

Study stations. In late winter/early spring of 2015 (14 March to 25 March) seawater sampling was conducted onboard the R/V *Sikuliaq* across the Gulf of Alaska into the Bering Sea (Figure 1). Sampling was designed to target eukaryotic microbial communities in the water column along a northern transect from open ocean conditions in the North Pacific into the ice-covered areas of the Bering Sea (Table 1). Sea ice sampling was conducted at one station to further assess diversity difference and serve as a standard reference for interpreting non-metric multidimensional scaling (NMDS) spatial plotting distance.

Sampling and sample processing. Three biological replicate samples were collected at five water stations and at a single sea ice station. A single replicate corresponded to a single Niskin bottle or a single 10-cm bottom ice core section. Water samples were collected using a CTD/Rosette sampler holding 24 10-liter Niskin bottles from the chlorophyll *a* maximum. The chlorophyll *a* maximum depth was identified with *in situ* readings of a CTD-mounted fluorometer (Seapoint) and targeted to reduce taxa abundance variability introduced with depth and algal biomass (e.g. Yasuhara et al. 2012; Nelson et al. 2014). All replicates at a sampling site were collected from a single CTD cast. For all water samples, corresponding triplicate nutrient samples (100 mL) were acquired for PO_4, $Si(OH)_4$, NO_3, NO_2, and NH_3 analysis.

One liter of water was collected per replicate immediately following CTD retrieval for sequencing analysis. Samples were separately filtered onto 0.6-µm DTTP filters (Millipore) using a vacuum filter onboard the R/V *Sikuliaq*. Samples were stored in sterile polypropylene tubes at −80°C onboard the R/V *Sikuliaq* and then at the University of Alaska Fairbanks until DNA extraction. At the Sea Ice station, three ice cores were extracted using a 9-cm diameter KOVACs ice corer. The bottom 10-cm of each core

was sectioned using an ethanol-sterilized handsaw. Ice core sections were melted at room temperature into 1000 mL of 0.22-µm-filtered seawater. After complete melt of the ice cores, samples were vacuum-filtered onto 0.6-µm DTTP filters (Millipore) and were stored in sterile polypropylene tubes at −80ºC onboard the R/V *Sikuliaq* and then at the University of Alaska Fairbanks until DNA extraction.

DNA extractions were conducted at the University of Alaska Fairbanks by bead beating for 1 minute in phosphate buffer, followed by phenol-chloroform extraction. Biological replicates were pooled before PCR. Target amplicons were generated using the Earth Microbiome Project primers: Euk_1391f: (5′-GTACACACCGCCCGTC-3′) and EukBr_1510r: (5′- TGATCCTTCTGCAGGTTCACCTAC-3 ′) (Stoeck et al. 2010) to generate ~170 base pair reads from the V9 region of the 18S rRNA subunit. Sequencing libraries were prepared using the TruSeq DNA Library Preparation Kit LT at Michigan State University following the manufacturer's protocol. HTS was conducted on an Illumina MiSeq v2 flow cell using paired-end reads. Samples were split according to location and multiplexed in a single MiSeq run. Base calling was performed by Illumina Real Time Analysis v1.18.54 and was demultiplexed and converted to FastQ files with Illumina Bcl2fastq v1.8.4.

Sequence analysis and processing was conducted using Mothur v1.33.3 (Kozich et al. 2013; Schloss et al. 2009). Sequences were aligned using the SILVA (Quast et al. 2013) reference database (Release 119), screened for chimeras (Edgar et al. 2011) and classified with SILVA (Release 119), using the K-nearest neighbor algorithm (bootstrap cutoff value of 80% following 1,000 iterations). Bacteria, Archaea and metazoans were removed from all data sets. Sequences were then clustered into operational taxonomic units (OTUs) at 97% similarity using the Average Neighbor distance. Datasets were normalized in Mothur (sub.sample) to the lowest number of sequences (62,588) for all downstream analyses.

Rarefaction curves were generated in Mothur (subsampling frequency of 500). To assess the OTU sampling coverage of normalized datasets, Good's non-parametric estimate of richness was used to assess success of sampling coverage using the 97% OTU definition. Richness, diversity, and evenness values were generated using the summary.single command. Taxonomic graphs representing eukaryotic supergroups were generated using the SILVA 119 classification and manually grouped to reflect recent eukaryotic taxonomy (Burki 2014). Based on this classification, the Cryptophyta, Picozoa, Kathablepharidae, Centrohelida, Haptophyta, and Telonema were grouped as *Incertae Sedis*. Ordination was conducted in R with the Vegan package using normalized OTU tables. For NMDS plots, Bray-Curtis distance was used to assess community dissimilarities (β-diversity) in two dimensions with minimal stress.

Results

Following sequence vetting and processing, 1,146,437 high-quality unique DNA sequence reads from the six stations were clustered into 14,874 OTUs that were used in downstream analysis. After data normalization in Mothur, 375,528 high quality sequences, corresponding to 14,510 unique OTUs, were used for comparative analysis. There was a sum total of 19,319 OTU observations in our normalized databases, including singleton OTUs and shared OTUs (i.e. repeat OTU observations between different sites) (Table 2). Sequencing depth from a single MiSeq run was sufficient to obtain >96% sample coverage across all sites (Table 2). This sequencing depth resulted in near-saturation of rarefaction curves (Online Resource 1).

In all water samples, the alveolates had the highest relative abundance among the eukaryotic supergroups, followed by stramenopiles and opisthokonts. In sea ice, the relative abundance of supergroup taxa was markedly different and was comprised of mostly the stramenopiles, followed by alveolates and rhizarians (Figure 2). Sites sampled in southwestern Alaska (Shelikof Strait and Deep Water Basin) had similar community relative abundance, despite substantial geographic distance (~800 km). While these sites had analogous community structure, Shelikof Strait had an additional 3,928 taxa. Chao1 estimates of species richness across all sites revealed that microbes within Shelikof Strait had the second highest estimated richness (6,840) and that the Deep Water Basin had the lowest (2,912). The low estimate of richness in the Deep Water Basin corresponded to the lowest number of observed OTUs (1,863). North of the Aleutian Islands, eukaryotic community structure varied with increasing latitude, even across short geographical distances (e.g. ~160 km between Pribilof Islands/Bering Sea Shelf sites). In the Bering Sea, Chao1 species richness increased with decreasing temperature, with the marginal ice zone (MIZ) (-1.7^{o}C) having the highest estimated OTU richness of all sites. Multidimensional scaling of samples illustrated the dissimilarity of community structure (Figure 3). β-diversity showed grouping between the two locations in southwestern Alaska (Deep Water Basin/Shelikof Strait). A second grouping consisted of the MIZ and Bering Shelf location, while the sea ice sample and Pribilof Island site were separate (Figure 3A).

We detected all major taxonomic supergroups (Online Resource 2), with a high diversity of dinoflagellates, diatoms, and ciliates. Functionally, there was a strong prevalence of fish and invertebrate symbionts (e.g. *Paramoeba branchiphila, P. eilhardi*, *Debaryomyces hansenii, Thalassomyces fagei, Pseudocollinia oregonensis,* and *Blastodinium navicula*), diatom parasites (e.g. chytrids and *Pirsonia* sp.) and toxin-producing phototrophs (e.g. *Alexandrium* sp., *Pseudo-nitzschia australis* and *Aureococcus*

anophagefferens) that have been reported from the Bering Sea and Arctic (e.g. Lewitus et al. 2012; Hassett and Gradinger 2016). A number of terrestrial organisms were detected at sampling stations, including Agaricomycetes and *Udeniomyces pannonicus*. Additionally, a number of cryptic clades were detected across our sample sites, including: nine Marine Stramenopile (MAST) clades, Novel Apicomplexa Class 2, DH147-EKD23 ciliate clade, SL163A10 Antarctic clade, SCM28C5, the NOR26, TAGIRI-17, D-52, FV36-2G-8, E222 and a number of clone-detected species (Online Resource 2).

Often, the greatest number of observed OTUs did not correspond to the highest richness estimate for a location (e.g. the Sea Ice station), largely explainable, as Chao1 is a non-parametric estimator of the minimal number of OTUs in a sample that is sensitive to singleton abundance. To this end, samples with a higher abundance of singletons have higher Chao1 estimates/extrapolations of species richness (Table 2). In order to supplement Chao1 estimates, the Simpson index was used to assess diversity. The Simpson index is the probability of the same taxon being chosen at random and increases as diversity decreases. The Simpson index is affected by the evenness of taxa in a sample; consequently, the Deep Water Basin had the lowest Simpson diversity (0.06) and the greatest evenness (0.008), while the Pribilof Islands with the highest Simpson diversity (0.21) was also the least even (0.0014).

To explore the relationship between inorganic nutrients and water masses in helping shape pelagic eukaryotic microbial community structure, NMDS ordination was employed to assess community dissimilarity and fitted with vectored nutrient data and water temperature (Figure 3B). R^2 values revealed that the majority of dimensional variability was explained by phosphate (R^2=0.93), silicate (R^2=0.99) and temperature (R^2=0.97) with a stress value of 7.71×10^{-5}, indicating a quality relationship for NMDS in two dimensions. The inorganic chemical signatures of structurally similar communities were analogous (Table 3) between grouped sites, with the exception of silicate. Silicate concentrations were lowest within the Bering Sea Shelf site and highest at the Pribilof Islands site. Silicate (NMDS, p=0.09) and phosphate (NMDS, p=0.12) values were not significant drivers of community structure. Decreasing water temperature across the south-north transect was a significant driver of microbial community structures (NMDS, p=0.03).

Comparative analysis of terminal sites (i.e. Shelikof Strait and the Sea Ice station) versus all other sites revealed a decreasing number of shared OTUs with increasing distance from terminal sites (Figure 4, Table 3). Water samples from the Bering Sea sites shared more OTUs with the Shelikof Strait site than with the sea ice sample, despite the existence of sea ice in the Bering Sea.

Discussion

185 The objective of this research was to explore general diversity patterns across the Alaskan Subarctic
186 marine system and to assess the effects of nutrients and geography in shaping eukaryotic microbial
187 communities in late winter. We detected a diverse eukaryotic microbial community across the shelf
188 ecosystem with Chao1 richness exceeding the estimated microbial richness of deserts (An et al. 2013),
189 coral reefs systems (Barott et al. 2011) and fungal diversity in rainforests (Paulus et al. 2006). Similarly,
190 these Bering Sea richness estimates exceed archaeal diversity in the coastal Arctic Ocean (Galand et al.
191 2006) and microbial communities in Arctic lakes (Galand et al. 2008).

192 We detected a diverse community of diatoms (~50% of established morphological inventories; Szymanski
193 and Gradinger 2016), dinoflagellates, and ciliates that are commonly found in the Bering Sea (e.g.
194 Howell-Kübler et al. 1996; Sorokin et al. 1996). We detected a number of common terrestrial organisms,
195 such as fungi that are common taxa found in permafrost (Gittel et al. 2014). The eastern Bering Sea, like
196 other shelf regions, receives a large amount of freshwater runoff from rivers, such as the Yukon River
197 (Mathis et al. 2011); consequently, we hypothesize that these organisms were sourced into the Bering Sea
198 from river runoff or eolian transport (Serno et al. 2014).

199 Assessing the true species richness of eukaryotes using HTS techniques is confounded by the application
200 of multiple species concepts across different eukaryotic clades (Grattepanche et al. 2014) and sequencing
201 errors (e.g. Bachy et al. 2013). For instance, diatom taxonomy employs a morphospecies concept that
202 does not correspond with the phylogenetic species concept (Moniz et al. 2010). We therefore suggest that
203 our species number estimate is likely incomplete for organisms defined by morphology. Additionally,
204 divergent paralogous evolution of 18S rRNA genes (Kondrashov et al. 2002; Alverson and Kolnick 2005)
205 can lead to overestimation of diversity. In some diatom species, intragenomic variation of 18S rRNA can
206 approach 2% divergence (Alverson and Kolnick 2005). To address these issues, we employed stringent
207 quality filtering of sequence reads and 3% similarity clustering to reduce overestimations of diversity.

208 When assessing community structure, we phylogenetically classified our sequences using an 80%
209 bootstrap cutoff and conservatively illustrated community structure by binning these classified sequences
210 into taxonomic supergroups (Figure 1) within a contemporary taxonomy paradigm. To assess similarities
211 of community composition more stringently, we conducted NMDS ordination using our normalized OTU
212 tables. Together these data depict the nearly-identical community structure of the Deep Water
213 Basin/Shelikof Strait and MIZ/Bering Sea Shelf stations (Figure 3A). In the southerly Deep Water
214 Basin/Shelikof Strait sites, ordinated grouping of sequence reads can be explained by the oceanographic
215 coupling between these two sites. Specifically, strong advection from the Alaska Coastal Current and the
216 Alaska Stream will produce similar water masses with related temperatures and salinity in regions south

of the Aleutian Islands. These similarities are heightened by reduced vertical mixing with increasing depth. The Shelikof Strait and the Deep Water Basin sites had similar temperatures that were the highest among all sites sampled (Table 1). Conversely, the MIZ and the Bering Sea Shelf stations had the coldest temperatures from any water column sites. We hypothesize that water mass similarities, as assessed by temperature and inorganic nutrient concentrations, resulted in structurally similar microbial communities, likely under comparable environmental selection pressures. The Pribilof Islands site was spatially ordinated between shallow northern cold water sites and deeper southern warm water sites. The Pribilof Islands receive a mixture of northerly advected Alaskan Coastal Current water and Aleutian North Slope Current (Aydin and Mueter 2007). We sampled in proximity to the transition zone between the middle and outer shelf domain; consequently, the Pribilof Island eukaryotic microbial community structure likely represents an intermediate wintertime community comprised largely of southerly taxa and some northerly taxa (Table 3).

Despite similar community structure, eukaryotic microbial community richness was markedly lower in the Deep Water Basin, relative to Shelikof Strait (Table 2). The richness differences between the southern Alaskan sites were largely driven by the abundance of singleton taxa. Analogous community structure, maintained by fewer individual taxa suggests diminished ecological redundancy in the Deep Water Basin, underscoring the susceptibility of microbial communities to climate change. Additional research exploring functional gene repertoires would help assess redundancy, gauge susceptibility of equilibrated communities, and monitor alternative stable-states of these communities.

Originally, we hypothesized that the eukaryotic microbial community structure would differ with hydrography. Within the wintertime Bering Sea, we found evidence that hydrography shapes large scale spatial diversity patterns of eukaryotic communities resulting in spatially-ordinated Bering Sea communities in sequential order of increasing latitude and estimated richness. This positive relationship between latitude and richness resulted in the MIZ having the highest estimated richness in the Bering Sea. The MIZ is a unique community composed of true pelagic organisms and those sourced from the sea ice (Moran et al. 2012). A number of taxa were only detected within both sea ice and the MIZ: Eugregarinorida, *Strombidinopsis* sp., *Euplotes charon, Maullinia ectocarpi, Guinardia delicatula, Rhizosolenia imbricate,* and the FV36-2G-8 clade. Consequently, we hypothesize that dual contributions from the pelagic and sea ice realm resulted in the highest Chao1 richness within the MIZ. By extension, the decreasing richness at the Bering Sea Shelf station and Pribilof Islands was likely influenced by ice cover and organisms seeded from the sea ice environment. Strong northerly winds can advect sea ice into the southeastern Bering Sea, ephemerally covering the Bering Sea Shelf station, as it did in 2015. We

hypothesize that this advection resulted in a mixture of taxa found only in sea ice, the MIZ and the Bering Sea Shelf site (e.g. SCM28C5 clade, *Eutintinnus* sp., *Paulinella chromatophora*, Globothalamea, Rotaliida, D52 clade); however, the shared number of OTUs between sea ice and other sites was minimal, relative to the Shelikof Strait site (Table 3). Consequently, we surmise that northward flowing warmer water mainly structures eukaryotic microbial communities in the Bering Sea in late winter. These communities can be marginally supplemented with taxa sourced from migrating sea ice. Furthermore, during this mixing of sea ice and Gulf of Alaska taxa, temperature helps select for species composition, supporting previous observations made in the Arctic Ocean (Lovejoy et al. 2006). Ultimately, our data suggest that temperature is a better indicator of eukaryotic microbial community structure than proximity to Bering Sea sea ice.

We hypothesized that the high concentrations of nitrate, silicate, and phosphate (among the highest in any marine system globally) within the Bering Sea (Whitledge and Luchin 1999) would be a driver for microbial community structure in wintertime. Analysis of nutrient data were within the historical ranges previously reported for nitrate (Sherr et al. 2013) and silicate (Tsunogai et al. 1979). Overall, we did not find evidence for the significant effects of nutrients on structuring microbial communities in wintertime, even by focusing our analysis on the chlorophyll maximum that is often dominated by photosynthetic diatoms that require inorganic silicate. Further research is needed to evaluate the synergism of nutrients (such as phosphate), temperature and seasonality in structuring microbial communities.

We believe that our data begin to delineate the Arctic-Subarctic ecotone region (Figure 4) of eukaryotic microbial communities in wintertime. This ecotone is defined by the spatial-temporal distribution of sea ice coverage that creates a gradient of cold water across the southeastern Bering Sea shelf. As solar irradiance increases in spring and stimulates the phytoplankton bloom, other factors such as light regime, stratification, and biological interactions will largely shape the eukaryotic community; however, in wintertime with overall low or non-existing new primary productivity, large scale diversity patterns appear to be driven by temperatures, irrespective of the unique chemical signatures across large geographical distances. Ultimately, our observations reinforce the coupled nature between physical oceanography and microbial diversity patterns and underscore the diversity responses of microbial communities to temperature. We suggest that an increase in microbial diversity studies would greatly benefit the understanding of biological responses to climate change by focusing on the base of food webs and the organisms that are likely to respond the quickest to abiotic perturbations.

The findings of this research are interesting and suggestive of important biological processes at the base of food webs. Our study targeted six unique geographical areas along a northwesterly transect that was focused on the chlorophyll maximum; consequently, these data offer preliminary evidence into the structure, richness, diversity, and distribution of eukaryotic microbes across the Bering Sea in wintertime. The findings from this work can inform more vigorous studies of Bering Sea microbial diversity and offer insights into the coupling of microbial diversity and ocean circulation patterns that should guide future research exploring functional redundancy and longitudinal diversity gradients.

Acknowledgements

Research design, experimentation, analyses, manuscript writing, manuscript formatting was conducted by Brandon T. Hassett. Manuscript editing and research design was conducted by Rolf Gradinger. This material is supported by National Science Foundation Award DGE-0801720,the Marine Ecosystem Sustainability in the Arctic and Subarctic (MESAS) IGERT #1303901. Sequence data has been deposited in the NCBI Sequence Read Archive under BioProject accession 305168. The funders had no role in study design, data collection and interpretation, or the decision to submit the work for publication.

Conflict of Interest.

The authors declare no conflict of interest.

297 **Works Cited**

298 Alverson AJ, Kolnick L (2005) Intragenomic nucleotide polymorphism among small subunit (18S) rDNA
299 paralogs in the diatom genus *Skeletonema* (Bacillariophyta). J Phycol 41:1248–1257

300 An S, Couteau C, Luo F, Neveu J, DuBow MS (2013) Bacterial diversity of surface sand samples from the
301 Gobi and Taklamaken Deserts. Microb Ecol 66:850–860

302 Aydin K, Mueter F (2007) The Bering Sea-A dynamic food web perspective. Deep-Sea Res Pt II 54:2501–
303 2525

304 Bachy C, Dolan JR, López-Garcia P, Deschamps P, Moreira D (2013) Accuracy of protest diversity
305 assessments: morphology compared with cloning and direct pyrosequencing of 18S rRNA genes
306 and ITS regions using the conspicuous tintinnid ciliates as a case study. ISME J 7:244-255

307 Barott KL, Rodriguez-Brito B, Janouškovec J, Marhaver KL, Smith JE, et al. (2011) Microbial diversity
308 associated with four functional groups of benthic reef algae and the reef-building coral
309 *Montastraea annularis*. Environ Microbiol 13:1192–1204

310 Burki F (2014) The eukaryotic tree of life from a global phylogenomic perspective. Cold Spring Harb
311 Perspect Biol 6:a016147–a016147

312 Carmack E, Barber D, Christensen J, Macdonald R, Rudels B, Sakshaug E (2006) Climate variability and
313 physical forcing of the food webs and the carbon budget on pan-Arctic shelves. Prog Oceanogr
314 71:145–181

315 Comeau AM, Li WKW, Tremblay JÉ, Carmack EC, Lovejoy C (2011) Arctic Ocean microbial community
316 structure before and after the 2007 record sea ice minimum. PLoS One.
317 doi:10.1371/journal.pone.0027492

318 Doney SC, Ruckelshaus M, Emmett Duffy J, Barry J, Chan F, et al. (2012) Climate change impacts on
319 marine ecosystems. Ann Rev Mar Sci 4:11–37

320 Edgar RC, Haas BJ, Clemente JC, Quince C, Knight R (2011) UCHIME improves sensitivity and speed of
321 chimera detection. Bioinformatics 27:2194–2200

322 Fossheim M, Primicerio R, Johannesen E, Ingvaldsen RB, Aschan MM, Dolgov AV (2015) Recent warming
323 leads to a rapid borealization of fish communities in the Arctic. Nat Clim Chang 5:1–6

324 Galand PE, Casamayor EO, Kirchman DL, Lovejoy C (2009) Ecology of the rare microbial biosphere of the
325 Arctic Ocean. PNAS 106:22427–22432

326 Galand P, Lovejoy C, Pouliot J, Garneau M, Vincent WF (2008) Microbial community diversity and
327 heterotrophic production in a coastal Arctic ecosystem: A stamukhi lake and its source waters.
328 Limnol Oceanogr 53:813–823

329 Galand P, Lovejoy C, Vincent WF (2006) Remarkably diverse and contrasting archaeal communities in a
330 large Arctic river and the coastal Arctic Ocean. Aquat Microb Ecol 44:115–126

331

Gittel A, Bárta J, Kohoutová I, Mikutta R, Owens S, et al. (2014) Distinct microbial communities associated with buried soils in the Siberian tundra. ISME J 8:841-853

Gradinger R (2009) Sea-ice algae: Major contributors to primary production and algal biomass in the Chukchi and Beaufort Seas during May/June 2002. Deep-Sea Res Pt II 56:1201–1212

Gradinger R, Bluhm B, Hopcroft R, Gebruk A, Kosobokova K, et al. (2010) Marine life in the Arctic. In: McIntyre A (ed) Life in the World's Oceans: Diversity, Distribution, and Abundance. Wiley-Blackwell, West Sussex, pp 183–202

Grattepanche JD, Santoferrara LF, McManus GB, Katz LA (2014) Diversity of diversity: Conceptual and methodological differences in biodiversity estimates of eukaryotic microbes as compared to bacteria. Trends Microbiol 22:432–437

Hassett BT and Gradinger R (2016) Chytrids dominate Arctic marine fungal communities. Environ Microbiol 18:2001-2009

Hassett BT, López JA, Gradinger R (2015) Two new species of marine saprotrophic sphaeroformids in the Mesomycetozoea isolated from the Sub-Arctic Bering Sea. Protist 166:310-322

Hodges LR, Bano N, Hollibaugh JT, Yager PL (2005) Illustrating the importance of particulate organic matter to pelagic microbial abundance and community structure - an Arctic case study. Aquat Microb Ecol 40:217–227

Holmes RM, McClelland JW, Peterson BJ, Tank SE, Bulygina E, et al. (2012) Seasonal and annual fluxes of nutrients and organic matter from large rivers to the Arctic Ocean and surrounding seas. Estuar Coast 35:369–382

Howell-Kübler AN, Lessard EJ, Napp JM (1996) Springtime microprotozoan abundance and biomass in the southeastern Bering Sea and Shelikof Strait, Alaska. J Plankton Res 18: 731-745

Kondrashov F, Rogozin I, Wolf Y, Koonin EV (2002) Selection in the evolution of gene duplications. Genome Biol 3:RESEARCH0008.1–0008.9

Kozich JJ, Westcott SL, Baxter NT, Highlander SK, Schloss PD (2013) Development of a dual-index sequencing strategy and curation pipeline for analyzing amplicon sequence data on the MiSeq Illumina sequencing platform. Appl Environ Microbiol 79:5112–5120

Leu E, Mundy C, Assmy P, Campbell K, Gabrielsen T, et al. (2015) Arctic spring awakening – steering principles behind the phenology of vernal ice algae blooms. Prog Oceanogr 139:1–31

Lewitus AJ, Horner RA, Caron DA, Garcia-Mendoza E, Hickey BM, et al. (2012) Harmful algal blooms along the North American west coast region: History, trends, causes and impacts. Harmful Algae 19:133-159

Lovejoy C, Massana R, Pedrós-Alió C (2006) Diversity and distribution of marine microbial eukaryotes in the Arctic Ocean and adjacent seas. Appl Environ Microbiol 72:3085–3095

366 Mathis JM, Cross JN, Bates NR (2011) Coupling primary production and terrestrial runoff to ocean
367 acidification and carbonate mineral suppression in the eastern Bering Sea. J Geophys Res 116:
368 C02030

369 Mueter FJ, Litzow M (2008) Sea ice retreat alters the biogeography of the Bering Sea continental shelf.
370 Ecol Appl 18:309–320

371 Moniz MBJ, Kaczmarska I (2010) Barcoding of diatoms: nuclear encoded ITS revisited. Protist 161:7–34

372 Moran SB, Lomas MW, Kelly RP, Gradinger R, Iken K, Mathis JT (2012) Seasonal succession of net
373 primary productivity, particulate organic carbon export, and autotrophic community
374 composition in the eastern Bering Sea. Deep-Sea Res Pt II 65-70:84–97

375 Nelson J, Ashjian C, Bluhm B, Conlan K, Gradinger R, et al. (2014) Biodiversity and biogeography of the
376 lower trophic taxa of the Pacific Arctic Region: sensitivities to climate change. In: Grebmeier J,
377 Maslowski W (ed) The Pacific Arctic Region: ecosystem status and trends in a rapidly changing
378 environment. Springer, Netherlands, pp 269–336

379 Paulus BC, Kanowski J, Gadek P, Hyde KD (2006) Diversity and distribution of saprobic microfungi in leaf
380 litter of an Australian tropical rainforest. Mycol Res 110:1441–1454

381 Piepenburg D, Archambault P, Ambrose WG, Blanchard AL, Bluhm B, et al. (2011) Towards a pan-Arctic
382 inventory of the species diversity of the macro- and megabenthic fauna of the Arctic shelf seas.
383 Mar Biodivers 41:51–70

384 Quast C, Pruesse E, Yilmaz P, Gerken J, Schweer T, et al. (2013) The SILVA ribosomal RNA gene database
385 project: improved data processing and web-based tools. Nucleic Acids Res 41:590–596

386 Roy K, Jablonski D, Valentine JW, Rosenberg G (1998) Marine latitudinal diversity gradients: tests of
387 causal hypotheses. PNAS 95:3699–3702

388 Schloss PD, Westcott SL, Ryabin T, Hall JR, Hartmann M, et al. (2009) Introducing Mothur: Open-source,
389 platform-independent, community-supported software for describing and comparing microbial
390 communities. Appl Environ Microbiol 75:7537–7541

391 Serno S, Winckler G, Anderson RF, Hayes CT, McGee D, et al. (2014) Eolian dust input to the Subarctic
392 North Pacific. Earth Planet Sci Lett 387:252–263

393 Sorokin YI, Sorokin PY, Mamaeva TI (1996) Density and distribution of bacterioplankton and planktonic
394 ciliates in the Bering Sea and North Pacific. J Plankton Res 18: 1-16

395 Stabeno P, Bond N, Kchel N, Salo S, Schumacher J (2001) On the temporal variability of the physical
396 environment over the south-eastern Bering Sea. Fish Oceanogr 10:81–98

397 Stabeno P, Schumacher J, Ohtani K (1999) The physical oceanography of the Bering Sea. In: Loughlin T,
398 Ohtani K (ed) Dynamics of the Bering Sea. University of Alaska Sea Grant, Fairbanks, pp 1–28

399 Steele M, Ermold W, Zhang J (2008) Arctic Ocean surface warming trends over the past 100 years.
400 Geophys Res Lett 35:1–6

401 Stoeck T, Bass D, Nebel M, Christen R, Jones MDM, et al. (2010) Multiple marker parallel tag
402 environmental DNA sequencing reveals a highly complex eukaryotic community in marine anoxic
403 water. Mol Ecol 19:21–31

404 Sherr EB, Sherr BF, Ross C (2013) Microzooplankton grazing impact in the Bering Sea during spring sea
405 ice conditions. Deep-Sea Res Pt II 94:57–67

406 Suttle CA (2007) Marine viruses--major players in the global ecosystem. Nat Rev Microbiol 5:801–812

407 Szymanski AJ, Gradinger R (2016) The diversity, abundance and fate of ice algae and phytoplankton in
408 the Bering Sea. Polar Biol 39: 309-325

409 Tsunogai S, Kisakabe M, Iizumi H, Hattori A (1979) Hydrographic features of the deep water of the Bering
410 Sea - The Sea of Silica. Deep-Sea Res 26:641–659

411 Whitledge T, Luchin V (1999) Summary of chemical distributions and dynamics in the Bering Sea. In:
412 Loughlin T, Ohtani K (ed) Dynamics of the Bering Sea. University of Alaska Sea Grant, Fairbanks, pp 217–
413 249

414 Yasuhara M, Hunt G, van Dijken G, Arrigo KR, Cronin TM, Wollenburg JE (2012) Patterns and controlling
415 factors of species diversity in the Arctic Ocean. J Biogeogr 39:2081–2088

416

417

418 **Supplemental Materials**

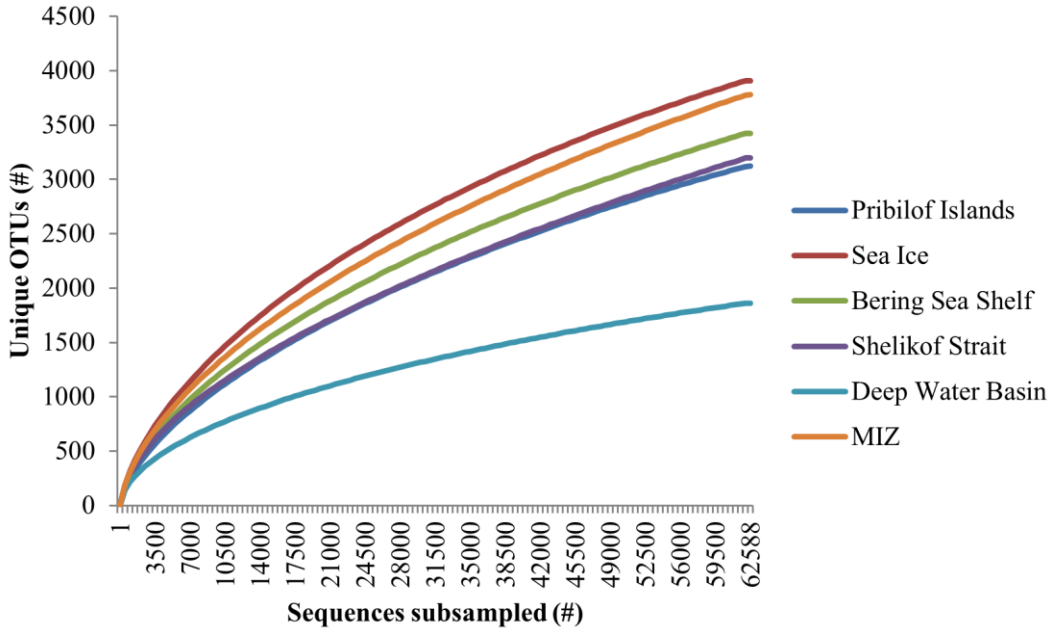

419

420 Online Resource 1. Sampling rarefaction curves. Curves were generated after sequence vetting,
421 subsampling (62,588) and clustering at 97% similarity, generated per site displaying the unique number
422 of OTUs per sampling effort.

423

Station Name	**PO_4**	***+/- s.d.***	**$Si(OH)_4$**	***+/- s.d.***	**NO_3**	***+/- s.d.***	**NO_2**	***+/- s.d.***	**NH_4**	***+/- s.d.***
Shelikof Strait	1.40	*0.31*	19.89	*4.70*	11.81	*3.36*	0.12	*0.05*	1.13	*1.96*
Deep Water Basin	1.31	*0.16*	20.88	*4.25*	12.18	*2.82*	0.09	*0.02*	0.008	*0.02*
Pribilof Islands	1.77	*0.35*	29.77	*7.43*	15.08	*4.72*	0.14	*0.07*	1.85	*3.21*
Bering Sea Shelf	1.23	*0.04*	18.57	*0.79*	9.43	*0.43*	0.10	*0.003*	4.0×10^{-5}	3.2×10^{-8}
MIZ	1.67	*0.17*	29.69	*3.61*	11.76	*1.68*	0.08	*0.02*	0.70	*1.2*

Table 3. Inorganic nutrient data (μM). Data was acquired from all water sites. Standard deviations (s.d.) are the result of three independent replicates.

Online Resource 2. Condensed taxonomy of detected organisms in the Bering Sea and surrounding areas. Organisms classified to minimally the taxonomic genus level are represented below. Select taxonomic clades in the Phaeophytes and fungi were represented by only sequences classifiable to Order and were included in this table. The majority of our sequences did not classify to the genus level and were not represented in this table. For example, the Prasinophytes were detected at every station, but *Prasinoderma sp.* is represented at only three stations.

	Shelikof Strait	Deep Water Basin	Pribilof Islands	Bering Sea Shelf	MIZ	Sea Ice
Amoebozoa						
Dactylopodids						
Paramoeba sp.	+	+	-	-	+	+
Paramoeba branchiphila	+	-	-	-	-	-
Paramoeba eilhardi	-	+	-	-	-	-
Tubulinds						
Vermamoeba sp.	+	-	-	-	-	-
Vermamoeba vermiformis	+	-	-	-	-	-
Paraflabellula hoguae	-	-	-	+	-	+
Excavata						
Diplonemids						
Diplonema sp.	-	-	+	-	-	-
Euglenids						
Petalomonas cantuscygni	+	-	-	-	-	-
Neobodo sp.	-	-	-	+	+	-
Ichthyobodo sp.	-	-	-	+	+	-
Archaeaplastida						
Prasinophytes						
Prasinoderma sp.	-	-	-	+	+	+
Opisthokonta						
Choanoflagellates						
Stephanoecidae	+	+	-	+	+	+
Diaphanoeca grandis	+	-	-	-	+	+
Mesomycetozoea						
Pseudoperkinsus tapetis	-	-	+	+	+	+
Fungi						
Chytrids						
Rhizophlyctidales	-	-	-	+	+	-
Ascomycota						
Capnodiales	-	-	-	-	+	-
Dothideales	+	-	-	-	-	-

Pleosporales	+	-	-	+	+	+

STable 4.1 continued…..

Penicillium sp.	+	-	+	-	-	-
Helotiales	+	+	+	+	+	-
Xylariales	-	+	+	+	+	-
Debaryomyces hansenii	-	-	+	-	-	-
Basidiomycota						
Agaricomycetes	-	+	+	-	-	-
Udeniomyces pannonicus	-	-	+	-	-	-
SAR						
Alveolates						
Apicomplexa						
Filipodium sp.	-	-	-	+	-	+
Gregarinidae sp.	-	-	-	-	+	+
Novel Apicomplexa Class 2	-	-	-	-	-	+
Ciliates						
DH147-EKD23	+	+	-	+	+	-
Pseudocollinia oregonensis	+	-	-	-	-	-
Peritrichia sp.	-	-	+	-	-	+
Scuticociliatia sp.	-	-	-	-	-	+
Mesanophrys carcini	-	-	-	-	-	+
Parauronema longum	-	-	-	-	-	+
Acineta sp.	-	-	-	-	-	+
Ephelota sp.	+	-	-	-	-	-
Cryptocaryon sp.	-	-	+	-	-	-
Loxophyllum sp.	-	-	-	-	+	-
Myrionecta	+	+	+	+	+	+
Eutintinnus sp.	-	-	-	+	+	+
Favella arcuata	-	-	-	-	-	+
Pelagostrobilidium sp.	+	+	+	-	+	-
Stenosemella sp.	+	+	-	+	+	+
Strombidinopsis sp.	-	-	-	-	+	+
Tintinnidium sp.	-	-	-	-	-	+
Tintinnidium mucicola	-	-	-	-	-	+
Tintinnopsis sp.	+	-	-	+	-	+
Tintinnopsis lohmanni	-	-	-	-	-	+
Tintinnopsis sp. JG-2-11a	+	-	-	+	-	+
Rimostrombidium veniliae	+	-	+	-	+	+
Discocephalus ehrenbergi	-	-	-	-	-	+
Euplotes sp.	+	-	-	-	+	+
Euplotes charon	+	-	-	-	+	+
Hypotrichia sp.	+	-	+	+	+	+

Hypotrichia sp. I-99	+	-	-	-	-	-
Holosticha sp.	-	-	-	+	-	-

STable 4.1 continued….

Oligotrichia	+	-	+	+	+	+
Laboea sp.	+	-	+	+	+	-
Pseudotontonia sp.	-	+	+	+	+	-
Strombidium sp.	+	+	+	+	+	+
Dinoflagellates						
Amphidinium sp.	+	+	+	+	+	-
Gymnodinium sp. CCMP422	-	-	-	+	-	-
Chytriodinium sp.	+	+	+	+	+	-
Lepidodinium sp.	+	+	-	-	-	-
Nematodinium sp.	-	-	+	-	-	-
Polykrikos sp.	-	-	-	-	-	+
Gyrodinium sp.	+	+	+	+	+	+
Azadinium sp.	+	-	-	-	-	-
Karlodinium veneficum	+	+	+	+	+	-
Pelagodinium beii	+	+	+	+	+	+
Symbiodinium sp.	+	+	+	-	-	-
Halostylodinium sp.	+	-	-	-	-	-
Alexandrium fundyense	+	+	+	+	-	+
Alexandrium ostenfeldii	+	-	+	+	-	+
Alexandrium tamarense	+	+	+	+	+	+
Ceratium tenue	+	+	+	+	+	+
Protoperidinium sp.	+	+	+	+	+	-
Protoceratium reticulatum	-	-	-	-	-	+
Scrippsiella sp.	-	-	-	+	-	+
Tintinnophagus acutus	-	-	-	-	-	+
Prorocentrum donghaiense	-	-	+	-	-	-
Prorocentrum minimum	+	+	+	+	+	-
SL163A10 (Antarctic)	+	+	+	-	+	-
Blastodinium navicula	+	-	-	+	-	-
Haplozoon sp.	+	+	+	+	+	-
Scrippsiella sp.	+	+	+	+	+	-
Paulsenella vonstoschii	-	-	-	-	-	+
Noctiluca scintillans	-	-	-	-	-	+
SCM28C5	-	-	-	+	+	+
Thalassomyces fagei	+	+	+	+	-	-
Eduboscquella crenulata	+	+	+	+	+	+
Takayama pulchellum	+	+	+	-	-	-
Syndiniales						
Amoebophrya sp.	+	-	+	+	+	+

Syndiniales Group I	-	+	+	+	+	+
Syndiniales Group II	+	+	+	+	+	-
Syndinium sp.	-	+	-	-	-	-

STable 4.1 continued….

Rhizaria						
Cercomonads						
Minchinia sp.	-	-	-	-	+	-
Cercozoa sp. CC-2--9d	-	-	-	+	-	-
Minorisa sp.	-	+	-	+	+	+
NOR26	+	+	+	+	+	-
Pseudopirsonia sp.	-	-	-	+	-	+
Nudifila sp.	-	-	-	-	-	+
Paulinella sp.	+	+	+	+	+	-
Paulinella chromatophora	-	-	-	+	+	+
Cryothecomonas sp.	+	+	+	+	+	+
Protaspa sp.	-	-	+	+	+	+
Ebria sp.	+	+	+	+	+	+
Thaumatomonads						
Thaumatomastix sp.	-	-	-	-	-	+
Phytomyxea						
Maullinia ectocarpi	-	-	-	-	+	+
Spongospora sp.	-	-	-	-	-	+
Paradinium						
Paradinium poucheti	-	-	+	-	-	-
Acantharia						
Acanthometra sp.	-	+	-	-	-	-
Uncultured marine acantharean DH147-EKD17	-	+	-	-	-	-
Chaunocanthida sp.	+	+	-	-	-	-
Foraminifera						
Globothalamea	-	-	-	+	+	+
Rotaliida	-	-	-	+	+	+
Polycystinea						
Lithomelissa setosa	+	+	+	-	-	-
Stramenopiles	-	+	+	+	+	+
Incertae Sedis						
Pirsonia sp.	+	-	+	+	+	+
Pirsonia guinardiae	+	-	+	-	-	+
Labyrinthulids						
D52	-	-	-	+	+	+
TAGIRI-17	-	-	-	-	-	+
Aplanochytrium sp.	-	-	-	+	-	+

MAST-1	-	+	-	+	+	+
MAST-2	+	+	+	+	+	+
MAST-3	+	+	+	+	+	+
MAST-4	+	+	+	+	+	-

STable 4.1 continued….

MAST-6	+	+	+	-	+	+
MAST-7	+	+	+	+	+	-
MAST-8	+	+	+	+	+	-
MAST-9	+	+	+	+	+	-
MAST-12	+	+	+	+	+	-
Chrysophytes						
Spumella sp.	+	-	-	-	-	+
E222	+	+	+	+	+	+
Ochromonas sp.	+	-	-	-	-	-
Chrysophyceae sp.	+	-	-	-	-	-
Diatoms						
Asterionellopsis glacialis	-	-	-	-	-	+
Asteroplanus karianus	+	+	+	+	+	+
Fragilariopsis sp.	+	+	+	+	+	+
Navicula sp.	-	-	+	-	-	+
Nitzschia sp.	+	+	+	+	+	+
Pleurosigma sp.	+	+	+	+	+	+
Pseudo-nitzschia australis	+	+	+	-	+	-
Attheya longicornis	+	+	+	+	+	+
Brockmanniella brockmannii	-	-	-	+	+	-
Chaetoceros sp.	+	+	+	+	+	+
Chaetoceros rostratus	+	+	+	+	+	+
Chaetoceros sp. CCAP 1-1-/16	-	-	-	+	-	-
Chaetoceros sp. p442	+	+	+	+	-	-
Cyclotella choctawhatcheeana	-	+	-	-	-	+
Cymatosira belgica	-	-	-	+	-	+
Ditylum brightwellii	+	+	+	+	+	-
Hyalosira sp. CCMP469	+	-	+	-	-	+
Minutocellus sp.	+	+	+	+	+	+
Porosira sp.	+	+	+	+	+	+
Skeletonema sp.	+	+	+	+	+	+
Thalassiosira sp.	+	+	+	+	+	+
Thalassiosira concaviuscula	+	-	+	+	+	-
Thalassiosira guillardii	+	-	-	-	-	+
Thalassiosira nordenskioeldii	-	-	-	-	-	+
Thalassiosira oceanica	-	-	-	+	-	-
Thalassiosira punctigera	+	+	+	-	-	-

Actinocyclus curvatulus	+	+	+	+	+	+
Corethron criophilum	+	+	+	+	+	-
Coscinodiscus radiates	+	+	+	-	+	-
Coscinodiscus sp. GGM-2—4	+	-	-	-	-	-
Melosira sp.	+	+	+	-	-	-

STable 4.1 continued…

Stephanopyxis nipponica	+	+	+	-	-	-
Leptocylindrus minimus	+	-	+	+	+	-
Proboscia alata	+	+	+	+	+	-
Guinardia delicatula	-	-	-	-	+	+
Rhizosolenia imbricate	-	-	-	-	+	+
Dictyochophytes						
Dictyocha speculum	+	+	+	+	+	-
Florenciella sp.	-	-	+	-	-	-
Pseudochattonella verruculosa	+	+	+	+	+	-
Apedinella radians	+	-	+	-	-	-
FV36-2G-8	-	-	-	-	+	+
Pseudopedinella elastica	+	-	+	+	-	-
Pteridomonas sp.	+	-	-	+	-	+
Pelagophytes						
Aureococcus anophagefferens	+	+	+	+	+	-
Pelagococcus subviridis	+	+	+	-	-	-
Pelagomonas calceolata	+	+	+	+	+	-
Phaeophytes						
Ectocarpales	-	-	-	-	-	+
Laminariales	-	-	-	-	-	+
Costaria costata	-	-	-	-	-	+
Peronosporomycetes						
Halocrusticida	-	-	-	-	-	+
Bolidomonas						
Bolidomonas pacifica	+	+	+	+	+	-
Incertae Sedis						
Cryptophytes						
Rhodomonas sp.	-	-	+	+	+	+
Teleaulax sp.	+	+	+	+	+	+
Kathablepharidae						
Katablepharis sp.	-	-	+	+	+	+
Leucocryptos sp.	-	-	-	+	-	-
Picozoa						
Picomonas sp.	+	+	+	+	+	-
Centrohelida						
Chlamydaster sterni	-	-	-	+	-	-

Haptophyta						
Emiliania huxleyi	+	+	-	-	+	-
Isochrysis galbana	+	-	-	-	-	-
Phaeocystis antarctica	+	+	+	+	+	-
Phaeocystis cordata	-	+	-	-	-	-
Chrysochromulina sp.	+	+	+	+	+	-

STable 4.1 continued

Chrysochromulina campanulifera	+	+	+	-	-	-
Chrysochromulina parva	+	+	+	-	-	-
Haptophytes						
Haptolina sp.	+	-	+	+	+	-
Telonema						
Telonema antarcticum	+	-	+	+	+	-